ARMY RESEARCH LABORATORY

Porous Thin Films Based on Photo-Cross-Linked Star-Shaped Poly(D,L-lactide)s

by Afia S. Karikari, Sharlene R. Williams, Cheryl L. Heisey, Adam M. Rawlett, and Timothy E. Long

ARL-RP-165 **March 2007**

A reprint from *Langmuir*, vol. 22, no. 23, pp. 9687–9693, November 2006.

NOTICES

Disclaimers

The findings in this report are not to be construed as an official Department of the Army position unless so designated by other authorized documents.

Citation of manufacturer's or trade names does not constitute an official endorsement or approval of the use thereof.

Destroy this report when it is no longer needed. Do not return it to the originator.

Army Research Laboratory
Aberdeen Proving Ground, MD 21005-5069

ARL-RP-165 **March 2007**

Porous Thin Films Based on Photo-Cross-Linked Star-Shaped Poly(D,L-lactide)s

Adam M. Rawlett
Weapons and Materials Research Directorate, ARL

Afia S. Karikari, Sharlene R. Williams, Cheryl L. Heisey, and Timothy E. Long
Virginia Polytechnic Institute and State University

A reprint from *Langmuir*, vol. 22, no. 23, pp. 9687–9693, November 2006.

REPORT DOCUMENTATION PAGE

Form Approved
OMB No. 0704-0188

1. REPORT DATE *(DD-MM-YYYY)*	2. REPORT TYPE	3. DATES COVERED (From - To)
March 2007	Reprint	June 2005–June 2006

4. TITLE AND SUBTITLE
Porous Thin Films Based on Photo-Cross-Linked Star-Shaped Poly(D,L-lactide)s

5a. CONTRACT NUMBER

5b. GRANT NUMBER

5c. PROGRAM ELEMENT NUMBER

6. AUTHOR(S)
Afia S. Karikari,* Sharlene R. Williams,* Cheryl L. Heisey,* Adam M. Rawlett, and Timothy E. Long*

5d. PROJECT NUMBER
AH84

5e. TASK NUMBER

5f. WORK UNIT NUMBER

7. PERFORMING ORGANIZATION NAME(S) AND ADDRESS(ES)
U.S. Army Research Laboratory
ATTN: AMSRD-ARL-WM-MA
Aberdeen Proving Ground, MD 21005-5069

8. PERFORMING ORGANIZATION REPORT NUMBER
ARL-RP-165

9. SPONSORING/MONITORING AGENCY NAME(S) AND ADDRESS(ES)

10. SPONSOR/MONITOR'S ACRONYM(S)

11. SPONSOR/MONITOR'S REPORT NUMBER(S)

12. DISTRIBUTION/AVAILABILITY STATEMENT
Approved for public release; distribution is unlimited.

13. SUPPLEMENTARY NOTES
A reprint from *Langmuir*, vol. 22, no. 23, pp. 9687–9693, November 2006.
*Virginia Polytechnic Institute and State University, Blacksburg, VA 24061

14. ABSTRACT
Self-assembly processes and subsequent photo-cross-linking were used to generate cross-linked, ordered microporous structures on the surfaces of well defined four-arm star-shaped poly(D,L-lactide) (PDLLA) thin films. The four-arm star-shaped PDLLAs were synthesized using an ethoxylated pentaerythritol initiator. Solutions of the PDLLAs were cast in a humid environment, and upon solvent evaporation, ordered honeycomb structures (or breath figures) were obtained. Correlations between molar mass, polymer solution viscosity, and pore dimensions were established. The average pore dimension decreased with increasing polymer solution concentration, and a linear relationship was observed between relative humidity and average pore dimensions. Highly ordered microporous structures were also developed on four-arm star-shaped methacrylate-modified PDLLA (PDLLA-UM) thin films. Subsequent photo-cross-linking resulted in more stable PDLLA porous films. The photo-cross-linked films were insoluble, and the honeycomb structures were retained despite solvent exposure. Free-standing, structured PDLLA-UM thin films were obtained upon drying for 24 h. Ordered microporous films based on biocompatible and biodegradable polymers, such as PDLLA, offer potential applications in biosensing and biomedical applications.

15. SUBJECT TERMS
breath figures, self assembly, hierarchical assembly

16. SECURITY CLASSIFICATION OF:			17. LIMITATION OF ABSTRACT	18. NUMBER OF PAGES	19a. NAME OF RESPONSIBLE PERSON
a. REPORT	b. ABSTRACT	c. THIS PAGE			Adam Rawlett
UNCLASSIFIED	UNCLASSIFIED	UNCLASSIFIED	UL	12	19b. TELEPHONE NUMBER (*Include area code*) 410-306-0695

Porous Thin Films Based on Photo-Cross-Linked Star-Shaped Poly(D,L-lactide)s

Afia S. Karikari,[†] Sharlene R. Williams,[†] Cheryl L. Heisey,[†] Adam M. Rawlett,[‡] and Timothy E. Long*,[†]

Department of Chemistry, Macromolecules and Interfaces Institute, Virginia Polytechnic Institute and State University, Blacksburg, Virginia 24061, and U. S. Army Research Laboratory, Aberdeen Proving Ground, Maryland 21005

Received January 31, 2006. In Final Form: July 31, 2006

Self-assembly processes and subsequent photo-cross-linking were used to generate cross-linked, ordered microporous structures on the surfaces of well defined four-arm star-shaped poly(D,L-lactide) (PDLLA) thin films. The four-arm star-shaped PDLLAs were synthesized using an ethoxylated pentaerythritol initiator. Solutions of the PDLLAs were cast in a humid environment, and upon solvent evaporation, ordered honeycomb structures (or breath figures) were obtained. Correlations between molar mass, polymer solution viscosity, and pore dimensions were established. The average pore dimension decreased with increasing polymer solution concentration, and a linear relationship was observed between relative humidity and average pore dimensions. Highly ordered microporous structures were also developed on four-arm star-shaped methacrylate-modified PDLLA (PDLLA-UM) thin films. Subsequent photo-cross-linking resulted in more stable PDLLA porous films. The photo-cross-linked films were insoluble, and the honeycomb structures were retained despite solvent exposure. Free-standing, structured PDLLA-UM thin films were obtained upon drying for 24 h. Ordered microporous films based on biocompatible and biodegradable polymers, such as PDLLA, offer potential applications in biosensing and biomedical applications.

Introduction

Hierarchically ordered porous films in the micrometer range are of significant interest for potential applications in various fields including membrane technologies[1] and microbiology.[2] Although many lithographic techniques[3−6] are known for the successful fabrication of porous thin films, the breath figure approach has received considerable interest due to the simple, inexpensive, and robust mechanism of pattern formation.[7−21] Breath figures are derived from ordered micrometer-sized water droplets that form during vapor condensation onto a polymer solution surface.[22] The process, also known as the solvent evaporation method, occurs as an appropriate solvent evaporates under humid conditions, leading to a temperature decrease at the air−liquid interface and subsequent water condensation.[23] The dropwise condensation proceeds in several steps. The first stage involves nucleation of the water droplets on the polymer solution surface. In the second stage, the droplets become large enough to eventually coalesce due to the self-similarity of the pattern and growth acceleration, subsequently leading to an ordering of the droplets into a hexagonal lattice.[24] The self-assembly of the water droplets into the hexagonal array corresponds to the lowest free energy state.[25] The temperature difference between the surface and the ambient conditions diminishes once the film surface is covered with water droplets. The high-density water droplets then descend into the polymer solution, and traces of the droplets are generated in the polymer matrix upon complete evaporation of the solvent, resulting in hexagonally ordered pores with a honeycomb structure.[26]

The simplicity of the breath figure pattern formation has led to the preparation of ordered porous films using a wide variety of polymers. Yabu and co-workers[7] recently prepared spherical and hemispherical micro lens arrays (MLAs) using honeycomb templates of poly(dimethylsiloxane) (PDMS) fabricated using

* Corresponding author. Telephone: +1-540-231-2480. Fax: +1-540-231-8517. E-mail address: telong@vt.edu.

[†] Virginia Polytechnic Institute and State University.

[‡] U. S. Army Research Laboratory.

(1) Yang, G.; Xiong, X.; Zhang, L. *J. Membr. Sci.* **2002**, *201*, 161−173.

(2) Nishikawa, T.; Nonomura, M.; Arai, K.; Hayashi, J.; Sawadaishi, T.; Nishiura, Y.; Hara, M.; Shimomura, M. *Langmuir* **2003**, *19*, 6193−6201.

(3) Petronis, S.; Gretzer, C.; Kasemo, B.; Gold, J. *J. Biomed. Mater. Res.* **2003**, *66A*, 707−721.

(4) Sirbuly, D. J.; Lowman, G. M.; Scott, B.; Stucky, G. D.; Buratto, S. K. *Adv. Mater.* **2003**, *15*, 149−152.

(5) Masuda, H.; Watanabe, M.; Yasui, K.; Tryk, D.; Rao, T.; Fujishima, A. *Adv. Mater.* **2000**, *12*, 444−447.

(6) Wu, M.; Park, C.; Whitesides, G. M. *J. Colloid Int. Sci.* **2003**, *265*, 304−309.

(7) Yabu, H.; Shimomura, M. *Langmuir* **2005**, *21*, 1709−1711.

(8) Stenzel-Rosenbaum, M. H.; Davis, T. P.; Fane, A. G.; Chen, V. *Angew. Chem., Int. Ed.* **2001**, *40*, 3428−3432.

(9) Francois, B.; Ederle, Y.; Mathis, C. *Synth. Metals* **1999**, *103*, 2362−2363.

(10) Zhao, B.; Li, C.; Lu, Y.; Wang, X.; Liu, Z.; Zhang, J. *Polymer* **2005**, *46*, 9508−9513.

(11) Hernandez-Guerrero, M.; Davis, T. P.; Barner-Kowollik, C.; Stenzel, M. H. *Eur. Polym. J.* **2005**, *41*, 2264−2277.

(12) Nygard, A.; Davis, T. P.; Barner-Kowollik, C.; Stenzel, M. H. *Aust. J. Chem.* **2005**, *58*, 595−599.

(13) Francois, B.; Pitois, O.; Francois, J. *Adv. Mater.* **1995**, *7*, 1041−1044.

(14) Srinivasarao, M.; Collings, D.; Philips, A.; Patel, S. *Science* **2001**, *292*, 79−82.

(15) Bolognesi, A.; Mercogliano, C.; Yunus, S.; Civardi, M.; Comoretto, D.; Turturro, A. *Langmuir* **2005**, *21*, 3480−3485.

(16) Widawski, G.; Rawiso, M.; Francois, B. *Nature* **1994**, *369*, 387−389.

(17) Cui, L.; Xuan, Y.; Li, X.; Ding, Y.; Li, B.; Han, Y. *Langmuir* **2005**, *21*, 11696−11703.

(18) Englert, B. C.; Scholz, S.; Leech, P. J.; Srinivasarao, M.; Bunz, U. H. F. *Chem-Eur. J.* **2005**, *11*, 995−1000.

(19) Song, L.; Bly, R. K.; Wilson, J. N.; Bakbak, S.; Park, J. O.; Srinivasarao, M.; Bunz, U. H. F. *Adv. Mater.* **2004**, *16*, 115−118.

(20) Yabu, H.; Takebayashi, M.; Tanaka, M.; Shimomura, M. *Langmuir* **2005**, *21*, 3235−3237.

(21) Cheng, C.; Tian, Y.; Shi, Y.; Tang, R.; Xi, F. *Macromol. Rapid Commun.* **2005**, *26*, 1266−1272.

(22) Noever, D. A. *J. Colloid Int. Sci.* **1995**, *174*, 92−96.

(23) Boker, A.; Lin, Y.; Chiapperini, K.; Horowitz, R.; Mark, T.; Carreeon, T.-X.; Abertz, C.; Skaff, H.; Dinsmore, A.; Emrick, T.; Russell, T. *Nature Mater.* **2004**, *3*, 302−306.

(24) Marcos-Martin, M.; Beysens, D.; Bouchaud, J. P.; Godreche, C.; Yekutieli, I. *Phys. A* **1995**, *214*, 396−412.

(25) Thomas, E. L.; Kinning, D. J.; Alward, D. B.; Henkee, C. S. *Macromolecules* **1987**, *20*, 2934−2939.

(26) Park, M. S.; Kim, K. K. *Langmuir* **2004**, *20*, 5347−5352.

10.1021/la0603020 CCC: $33.50
Published on Web 10/13/2006 PAGE EST: 6.8

the solvent evaporation method and the hemispherical MLAs exhibited improved projection properties relative to the spherical MLAs. In another study,[8] honeycomb structures were prepared using six-arm star polystyrene (PS), and a strong correlation between the number of arms, arm length, end-group functionality, and pore diameter were demonstrated. Other polymers that were used for the fabrication of honeycomb structures have included random and block copolymers of polystyrene (PS),[9−16,23] poly(2-vinyl pyridine) (P2VP),[17] poly(*p*-phenyleneethynylene) (PPE),[18,19] fluorinated PMMA copolymers,[20] and an amphiphilic copolymer containing dendronized poly(alkyl methacrylate) and linear poly(ethylene oxide) blocks.[21] The exploitation of a wide range of polymers for the successful fabrication of microporous structures using the breath figure methodology continues to generate considerable interest, and recent efforts are now focused on developing such patterned porosity on biocompatible polymers.

The use of biocompatible and biodegradable polymers for the fabrication of microporous surfaces using the solvent evaporation technique is especially advantageous for biomedical applications. Potential biomedical applications include electrochemical sensors for the analysis of blood electrolyte and glucose concentrations, immunosensors for the identification and quantification of biochemical substances, and scaffolds for tissue engineering.[27−29] Recently, honeycomb structures were fabricated on linear poly(ϵ-caprolactone), and the patterned films were reportedly useful for neural tissue engineering.[30] In another study,[31] porous films were prepared from random copolymers of polylactic acid and polyglycolic acid (poly(D,L-lactic acid-*co*-glycolic acid)) with different hydrophilicity values and a strong correlation between pattern formation and hydrophilicity was demonstrated. Honeycomb patterned films were also developed from a lactose-containing polymer, and gelatin, which is a cell adhesive ligand, was introduced onto the films. The gelatin immobilized porous films were bioactive and useful for cell culturing.[32,33] Fukuhira et al.[34] recently reported biodegradable honeycomb patterned films composed of poly(lactic acid) and dioleoylphosphatidylethanolamine (DOPE), a naturally derived phospholipid containing unsaturated fatty acid moieties. The patterned films demonstrated good cell proliferation and were promising candidates for scaffolds in tissue engineering applications.

Although patterned porous films developed using the breath figure method continue to generate considerable interest, their use in material and bioanalytical applications are limited due to their solubility in organic solvents. Recent efforts have subsequently focused on utilizing chemical and cross-linking techniques to obtain permanent honeycomb-structured films. Cross-linking techniques are expected to result in honeycomb-structured films with higher chemical and thermal stabilities, as well as higher mechanical strengths for further material patterning. Shimomura et al.[35] reported the fabrication of honeycomb structures on a cross-linked polyimide film and showed that the textured film retained the honeycomb structure when annealed at 300 °C. The honeycomb structures were first developed on a polyamic acid complexed with a diakylammonium salt, and the precursor film was then converted to the polyimide film through imidization. In another study, Bunz et al.[36] prepared honeycomb porous structures on an azide-substituted poly(*p*-phenyleneethynylene). After the structured film was thermally cross-linked at 300 °C, the polymer scaffold softened and collapsed to generate a thinner insoluble film with isolated holes that resembled a microfabricated "picoliter beaker."

The synthesis and photo-cross-linking of functionalized polymers has received much attention in our laboratories.[37−39] We also recently reported the synthesis and characterization of well-defined methacrylated four-arm star-shaped poly(D,L-lactide)s and subsequent photo-cross-linking to yield highly cross-linked networks with good mechanical properties for use as potential bioadhesives.[40] Herein, we demonstrate the first honeycomb microporous structures on well-defined methacrylated four-arm star-shaped poly(D,L-lactide)s containing an adjacent urethane site and subsequent photo-cross-linking to render the structures insoluble. The four-arm star PDLLAs were synthesized using a PEG-based macroinitiator, pentaerythritol ethoxylate. Photoreactive methacrylated end groups were obtained via functionalization of the hydroxyl-terminated star polymers with 2-isocyanatoethyl methacrylate (IEM), which also incorporated an adjacent urethane site to enhance the mechanical performance of the structured films through peripheral hydrogen bonding interactions. Free-standing, insoluble, honeycomb-structured thin films were obtained upon photo-cross-linking and extraction in chloroform. Atomic force and scanning electron microscopy were used to analyze the patterned PDLLA thin films.

Experimental Section

Synthesis and Modification of Four-Arm Star-Shaped PDLLA. Hydroxyl-terminated four-arm star-shaped PDLLAs of various molar masses ($<M_w>$ = 25 000, 36 000, and 58 000 g/mol) were synthesized and subsequently functionalized with IEM to obtain photoreactive methacrylate end groups with an additional urethane site as reported previously.[40]

Porous Honeycomb-Structured PDLLA Film. A humidity chamber with 65−90% relative humidity was prepared using a polycarbonate desiccator with a nitrogen inlet and outlet. Deionized water was placed in the chamber at ambient temperature, and nitrogen was bubbled through the water at a controlled rate. The gas velocity was regulated to control the relative humidity, and a digital Dickson hygrometer was used to measure the humidity in the chamber. The four-arm star-shaped PDLLA (0.5 g) was weighed in a sample vial and dissolved in dry CH_2Cl_2 to prepare 1.0−10 wt % polymer solutions. A photoinitiator, 2,2-dimethyl-2-phenol acetophenone (DMPA, 4 wt %, Aldrich), was added to the IEM-functionalized PDLLA star (PDLLA-UM) solutions prior to cross-linking. The substrate, a Dupont Kapton polyimide film (thickness 127 μm), was cut to the required size, rinsed twice with methanol, and dried with nitrogen. The Kapton substrate was taped to a glass microscope slide and then positioned in the humidity chamber. A few drops of PDLLA or PDLLA-UM solution were placed on the substrate in the humidity chamber, and the solvent was allowed to evaporate at room temperature at the specified relative humidity (RH).

Photo-Cross-Linking. The microporous PDLLA-UM films were passed through a Fusion UV system (model LC-6B benchtop

(27) Madou, M., *Fundamentals of microfabrication*; CRC Press: Boca Raton, FL, 1997.
(28) Ward, J. H.; Bashir, R.; Peppas, N. A. *J. Biomed. Mater. Res.* **2001**, *56*, 351−360.
(29) Neuman, M. R., Biomedical Sensors. In *The biomedical engineering handbook*; Bronzino, J. D., Ed. CRC Press: Boca Raton, FL, 1995; pp 779−787.
(30) Tsuruma, A.; Tanaka, M.; Fukushima, N.; Shimomura, M. *e-J. Surf. Sci. Nanotechnol.* **2005**, *3*, 159−164.
(31) Zhao, X.; Cai, Q.; Shi, G.; Shi, Y.; Chen, G. *J. Appl. Polym. Sci.* **2003**, *90*, 1846−1850.
(32) Nishida, J.; Nishikawa, K.; Nishimura, S.; Wada, S.; Karino, T.; Nishikawa, T.; Ijiro, K.; Shimomura, M. *Polym. J.* **2002**, *34*, 166−174.
(33) Nishikawa, T.; Nishida, J.; Ookura, R.; Nishimura, S.; Wada, S.; Karino, T.; Shimomura, M. *Mater. Sci. Eng. C* **1999**, C8−C9, 495−500.
(34) Fukuhira, Y.; Kitazono, E.; Hayashi, T.; Kaneko, H.; Tanaka, M.; Shimomura, M.; Sumi, Y. *Biomaterials* **2006**, *27*, 1797−1802.
(35) Yabu, H.; Tanaka, M.; Ijiro, K.; Shimomura, M. *Langmuir* **2003**, *19*, 6297−6300.
(36) Erdogan, B.; Song, L.; Wilson, J. N.; Park, J. O.; Srinivasarao, M.; Bunz, U. H. F. *J. Am. Chem. Soc.* **2004**, *126*, 3678−3679.
(37) Trenor, S. R.; Long, T. E.; Love, B. J. *J. Adhes.* **2005**, *81*, 213−229.
(38) Trenor, S. R.; Long, T. E.; Love, B. J. *Eur. Polym. J.* **2005**, *41*, 219−224.
(39) Trenor, S. R.; Long, T. E.; Love, B. J. *Macromol. Chem. Phys.* **2004**, *205*, 715−723.
(40) Karikari, A. S.; Edwards, W. F.; Mecham, J. B.; Long, T. E. *Biomacromolecules* **2005**, *6*, 2866−2874.

Scheme 1. Synthetic Methodology for the Preparation of Four-Arm, Star-Shaped, PDLLA, and Subsequent Functionalization with IEM (PDLLA-UM)

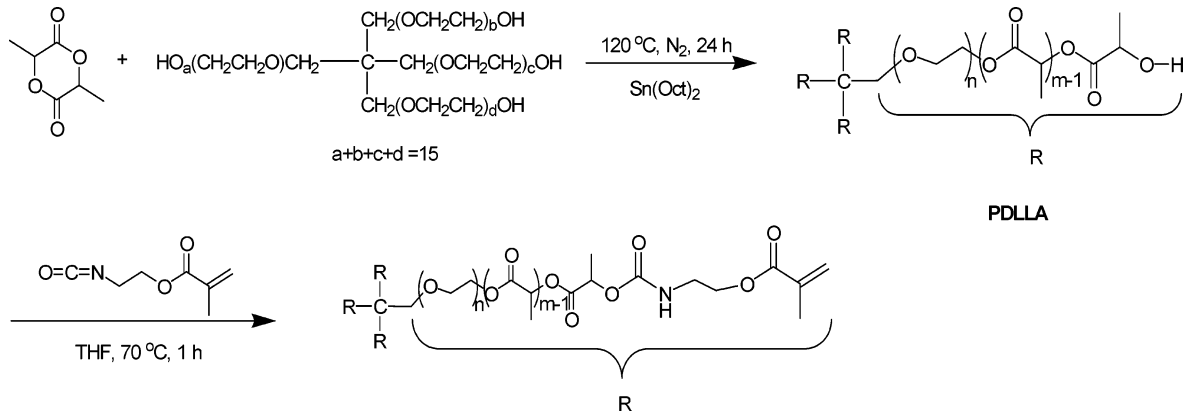

conveyor) at various belt speeds and energy doses to achieve photo-cross-linking. The irradiance and energy density were measured with an EIT UV Power Puck radiometer. The free-standing structured films were placed in chloroform for 2 h, and the gel content was determined gravimetrically.

Characterization. *Nuclear Magnetic Resonance Spectroscopy.* The polymer composition, number average molar mass, and percent functionalization were determined using ^{1}H NMR spectroscopy. The spectra were obtained using a Varian UNITY Spectrometer operating at 400 MHz using $CDCl_3$ as the solvent.

Size Exclusion Chromatography. Molar masses and molar mass distributions were determined at 40 °C in THF (ACS grade) at a flow rate of 1 mL/min using polystyrene standards on a Waters Alliance SEC system equipped with a Waters 2410 refractive index detector, a Wyatt Technology MiniDAWN MALLS detector, and a Viscotek 270 viscosity detector. Reported weight average molar masses are based on absolute measurements using the MALLS detector.

Atomic Force Microscopy. Pore depth and diameter were analyzed with a Dimension 3100 AFM equipped with a Nanoscope IV scanning probe microscope controller. Tap 300 Si_3N_4 tips with a spring constant of 40 N/m and set point to free amplitude ratio of 0.5 to 0.6 were used.

Scanning Electron Microscopy. The pore diameter and morphology were analyzed using a Leo 1550 field emission scanning electron microscope (FESEM). Microporous structures for FESEM analysis were collected on a $^1/_4$ in. × $^1/_4$ in. stainless steel mesh, mounted on a SEM disk, and sputter-coated with a 10 nm Pt/Au layer to reduce electron charging.

Results and Discussion

Well-defined four-arm star-shaped PDLLAs ($<M_w>$ = 25 000, 36 000, and 58 000 g/mol, and M_w/M_n = 1.16, 1.16, and 1.21, respectively) were prepared using pentaerythritol ethoxylate to initiate the ring-opening polymerization of DLLA as previously reported (Scheme 1).[40] Parameters such as polymer solution concentration, polymer molar mass, and humidity level are known to affect pattern formation of porous films developed using the solvent evaporation method[41] and these parameters were initially optimized using nonfunctionalized PDLLA solutions. The measured film thicknesses were 44, 48, and 61 μm for star-shaped PDLLA $<M_w>$ = 25 000, 36 000, and 58 000 g/mol, respectively.

Disordered microporous films with a random distribution of pore sizes were obtained at a 1.0 wt % PDLLA solution concentration (58 000 g/mol) while significant improvement in the pattern formation was observed as the polymer solution concentration was increased to 7.0 wt % (Figure 1a−d). At 1.0 wt %, condensed water droplets coalesced as the polymer solution viscosity was too low to stabilize the water droplets on the solution surface. The lack of coalescence at 7.0 wt % (Figure 1d) was attributed to a weakening of the thermocapillary convection responsible for convective motion in and between the two bodies of fluid.[42] As the PDLLA solution concentration was increased to 7.0 wt %, the solution viscosity increased, causing the convection patterns to disappear. The disappearance of the convection patterns combined with the highly viscous polymer film between the drops stabilized the condensed water droplets and resulted in highly ordered structures with monodisperse pore dimensions.[43,44]

The PDLLA solution concentration also influenced the shape of the pores in the structured films. Polygon-structured pores with a random distribution of pore dimensions were observed at 1.0 wt % (Figure 1a). Polygon-shaped pores were obtained at 1.0 wt % since the water droplets were presumed to coalesce only to a limited extent.[45] At high concentrations, the viscosity of the polymer solution dictates both the pore diameter and shape.[45] Hence the solution surface was stabilized at concentrations of 5.0 to 7.0 wt % due to the high surface tension at the water/organic solvent interface, and round highly ordered pores with mostly monodisperse pore dimensions were obtained.

The pore size decreased with increasing polymer solution concentration, and AFM was used to further probe the effect of polymer solution concentration on the pore dimensions.

The AFM results were consistent with the SEM results as shown in Figure 2. The average pore diameter measured using AFM section analysis (Figure 3) decreased from 6.2 to 4.7 μm as the concentration was increased from 1.0 to 7.0 wt % (Figure 4), while the average pore depth remained constant at about 2.0 μm. This decrease in average pore diameter was attributed to the increase in polymer solution concentration and viscosity.

The honeycomb wall surrounding the pores was thicker at the higher polymer solution concentrations and viscosities, and higher viscosities also prevented the condensed water droplets from sinking into the solution surface.[46] At low concentrations, however, the honeycomb wall was thinner due to decreased polymer solution viscosity and a reduction in the amount of

(41) Peng, J.; Han, Y.; Yang, Y.; Binyao, L. *Polymer* **2004**, *45*, 447−452.
(42) Aversana, P. D.; Banavar, J. R.; Koplik, J. *Phys. Fluids* **1996**, *8*, 15.
(43) Haupt, M.; Miller, S.; Sauer, R.; Thonke, K.; Mourran, A.; Moeller, M. *J. Appl. Phys.* **2004**, *96*, 3065−3069.
(44) Aversana, P. D.; Tontodonato, V.; Carotenuto, L. *Phys. Fluids* **1997**, *9*, 2475.
(45) Yu, C.; Zhai, J.; Gao, X.; Wan, M.; Jiang, L.; Li, T.; Li, Z. *J. Phys. Chem. B* **2004**, *108*, 4586−4589.
(46) Maruyama, N.; Karthaus, O.; Ijiro, K.; Shimomura, M.; Koito, T.; Nishimura, S.; Sawadaishi, T.; Nishi, N.; Tokura, S. *Supramol. Sci.* **1998**, *5*, 331−336.

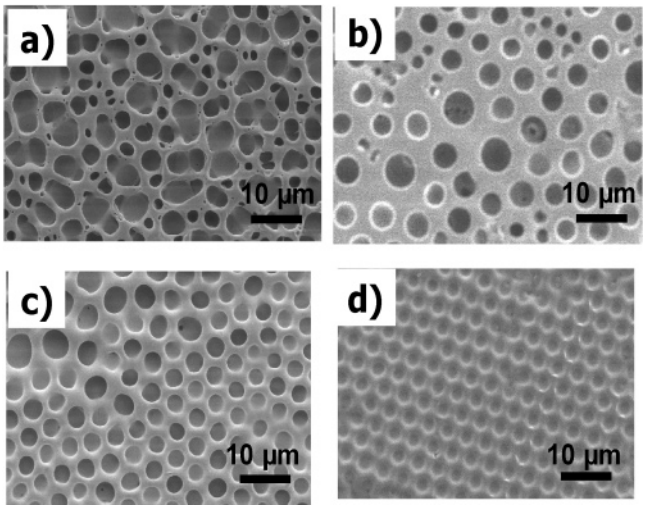

Figure 1. SEM images of microporous structures developed on the surfaces of nonfunctionalized star-shaped PDLLA ($<M_w> = 58\,000$ g/mol) at 76% RH and (a) 1.0, (b) 3.0, (c) 5.0, and (d) 7.0 wt % solution concentrations.

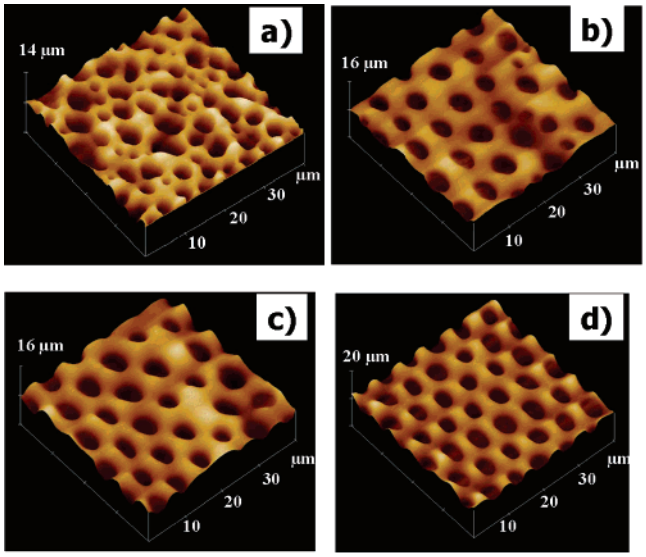

Figure 2. AFM images of microporous structures developed on the surfaces of nonfunctionalized star-shaped PDLLA ($<M_w> = 58\,000$ g/mol) at 76% RH and (a) 1.0, (b) 3.0, (c) 5.0, and (d) 7.0 wt % solution concentrations.

sample present in solution. Consequently, the condensed water droplets coalesced, resulting in larger pore diameters. The improved microporous film morphology with increased polymer solution concentration was therefore consistent with the roles of adequate polymer concentration and solution viscosity in preventing the coalescence of water droplets through efficient adsorption at the water/polymer interface.[47]

The arrangement of condensed water droplets as well as the size of the droplets contributed significantly to the pore size of the honeycomb film. As a consequence, atmospheric humidity was an important factor in the fabrication of porous films and influenced the condensation at the air−polymer interface and consequently affected pore size and the regularity of the pattern formation.[48] We observed significant improvement in the structured film morphology of nonfunctionalized PDLLA films

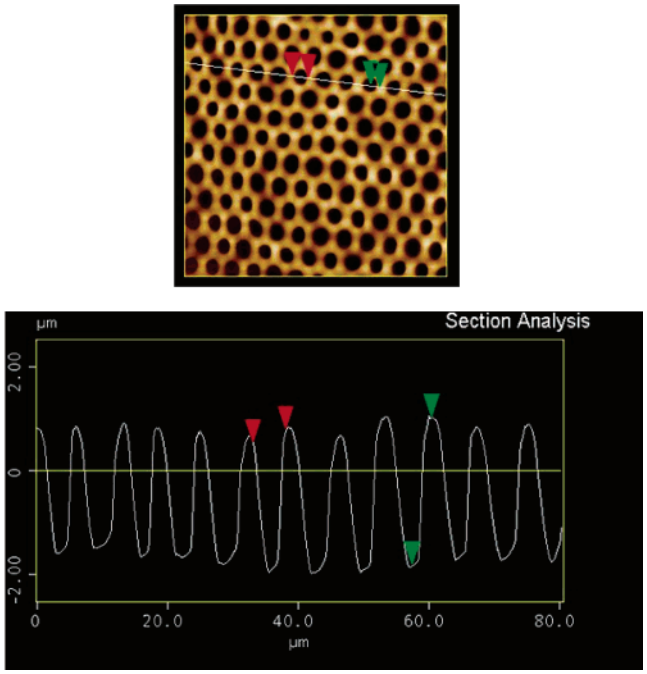

Figure 3. Top view and cross-sectional analysis of PDLLA (58 000 g/mol, 7.0 wt %) microporous structures prepared at 76% RH.

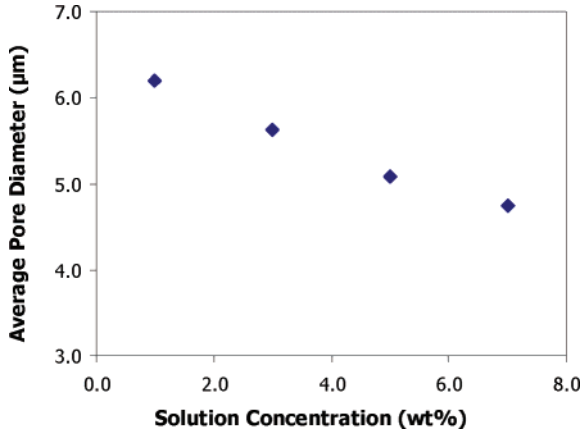

Figure 4. Plot illustrating the correlation between polymer solution concentration and average pore diameter. (Standard deviations ranged from 1.1 to 0.5 μm as the polymer solution concentration was increased from 1.0 to 7.0 wt %.)

(7 wt %, 58 000 g/mol) as the RH was increased from 66 to 86% (Figures 5 and 6). Irregular pores were obtained at 66% RH while the pattern formation was more controlled at 76 to 86% RH resulting in highly ordered porous films.

Pore diameter and depth increased with increasing RH, and this was attributed to the larger water droplets in equilibrium at higher relative humidity.[49] The average pore diameter increased from $1.5 \pm 0.2\,\mu$m to $5.3 \pm 0.6\,\mu$m while the average pore depth increased from $0.7 \pm 0.3\,\mu$m to $3.1 \pm 0.4\,\mu$m as the RH was increased from 66 to 86% RH (Figure 7).

The results therefore suggested that humidity levels in the range of 76−86% RH were required to successfully develop highly ordered microporous thin films. Previous reports have shown that low RH (<40%) resulted in the absence of porous structures, while at higher humidity (RH > 90), disordered coalesced pores were usually obtained due to rapidly condensing water droplets.[41]

(47) Karthaus, O.; Maruyama, N.; Cieren, X.; Shimomura, M.; Hasegawa, H.; Hashimoto, T. *Langmuir* **2000**, *16*, 6071−6076.
(48) Cheng, C. X.; Tian, Y.; Shi, Y. Q.; Tang, R. P.; Xi, F. *Langmuir* **2005**, *21*, 6576−6581.
(49) Connal, L. A.; Gurr, P. A.; Qiao, G. G.; Solomon, D. H. *J. Mater. Chem.* **2005**, *15*, 1286−1292.

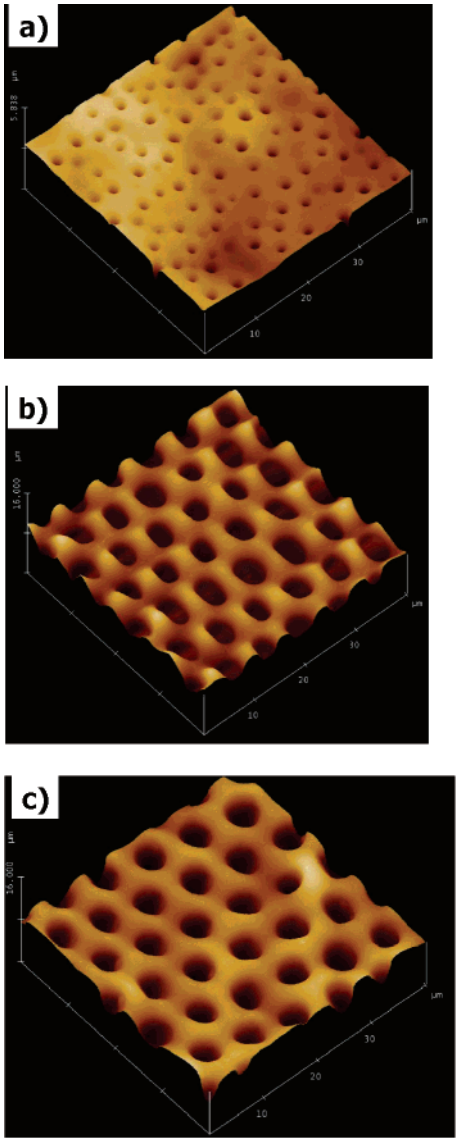

Figure 5. AFM images of microporous structures developed on the surfaces of nonfunctionalized star PDLLA (58 000 g/mol, 7.0 wt %) at RH of (a) 76 and (b) 86%.

The influence of star PDLLA molar mass on microporous structure formation and pore dimensions was evaluated using 7.0 wt % PDLLA/CH_2Cl_2 solutions with star PDLLA of 25 000, 36 000 and 58 000 g/mol $<M_w>$. A few drops of each solution were deposited on a Kapton substrate in an 86% RH humidity chamber to obtain thin porous films. Pores were formed on the 36 000 and 58 000 g/mol PDLLA, however, pores were not observed for the 25 000 g/mol polymer.

The solution viscosity (7.0 wt % in CH_2Cl_2) ranged from 4.5 to 14 cP as the PDLLA molar mass was increased from 25 000 g/mol to 58 000 g/mol (Figure 8). Microporous structures were not formed on the 25 000 g/mol PDLLA since the polymer solution viscosity was too low. The 36 000 g/mol PDLLA solution was more viscous, and the solution surface was able to support the condensed water droplets. Consequently, pores were formed after complete evaporation of the water (Figure 9a). However, the microporous pattern was irregular since the viscosity was still too low to prevent coalescence of the droplets suggesting that a higher molar mass was needed for higher ordering of the pores. At 58 000 g/mol, the increased polymer solution viscosity stabilized the polymer solution surface and prevented coalescence of the condensed water droplets leading to highly ordered

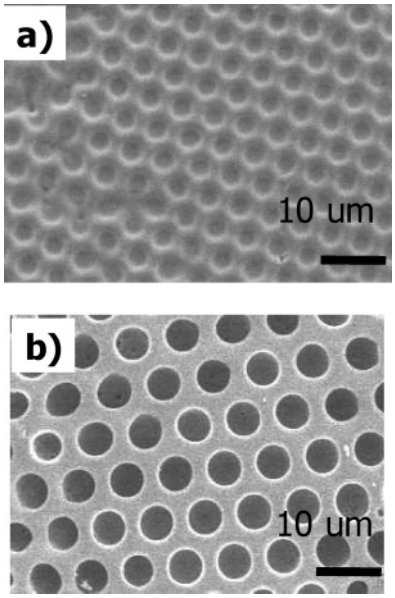

Figure 6. SEM images of microporous structures developed on the surfaces of nonfunctionalized star PDLLA (58 000 g/mol, 7.0 wt %) at (a) 76 and (b) 86% RH.

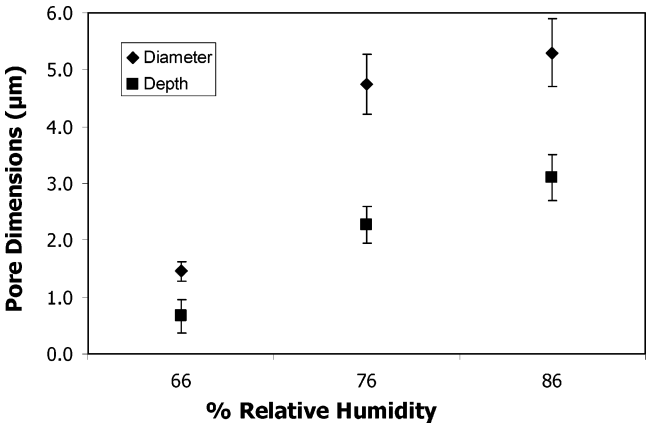

Figure 7. Correlation between relative humidity and PDLLA pore dimensions.

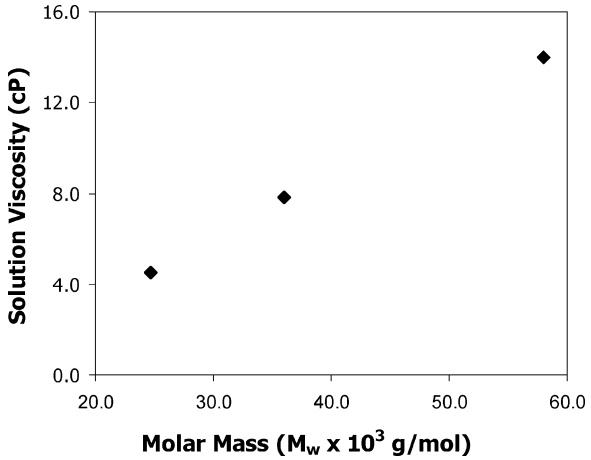

Figure 8. Solution viscosity (7.0 wt % in CH_2Cl_2) as a function of PDLLA molar mass.

structures with monodisperse pore dimensions (Figure 9b). It is also noted that precipitation of the polymer at the interface between the polymer solution and water creates a solid polymer envelop around the isolated water droplets and hence, stabilizes the water droplets and prevents coalescence.[50] Thus, earlier precipitation

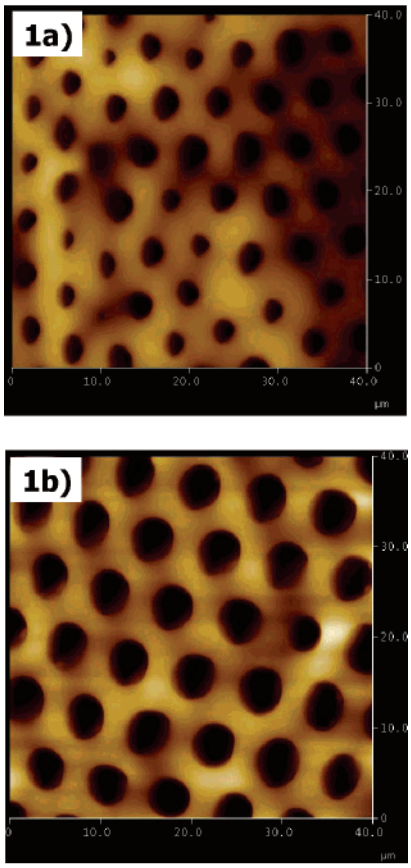

Figure 9. AFM images of microporous thin films developed at 86% RH on 7.0 wt % solutions of nonfunctionalized star PDLLA of (a) $<M_w>$ = 36 000 g/mol and (b) $<M_w>$ = 58 000 g/mol.

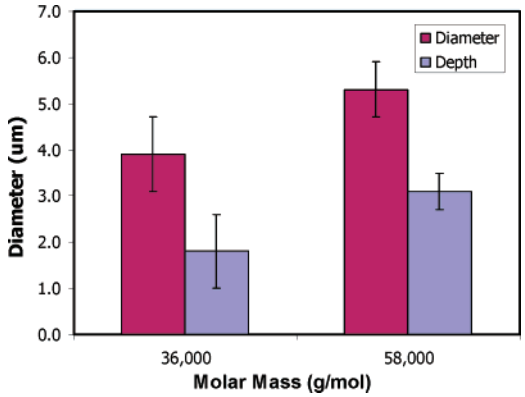

Figure 10. Plot illustrating the effect of increasing PDLLA molar mass on the average pore diameter.

at increasing PDLLA molar mass is expected to contribute to the improvement in the pattern formation.

In a consistent fashion as the earlier literature,[51−53] the average pore diameter and depth increased linearly with polymer molar mass (Figure 10). The pore diameter increased from 3.9 ± 0.8 μm to 5.3 ± 0.5 μm (Figure 10), while the pore depth increased from 1.8 ± 0.8 μm to 3.1 ± 0.4 μm as the molar mass was increased from 36,000 to 58,000 g/mol.

IEM was quantitatively reacted with the terminal hydroxyl groups of the star PDLLA (58,000 g/mol) in solution to obtain

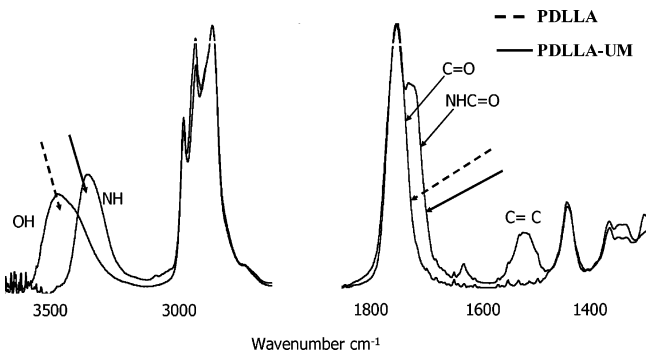

Figure 11. Stacked FT-IR spectra of four-arm star PDLLA and PDLLA-UM illustrating the disappearance of the OH group in the PDLLA and the appearance of the NH, NHC═O, and C═C groups in the PDLLA-UM.

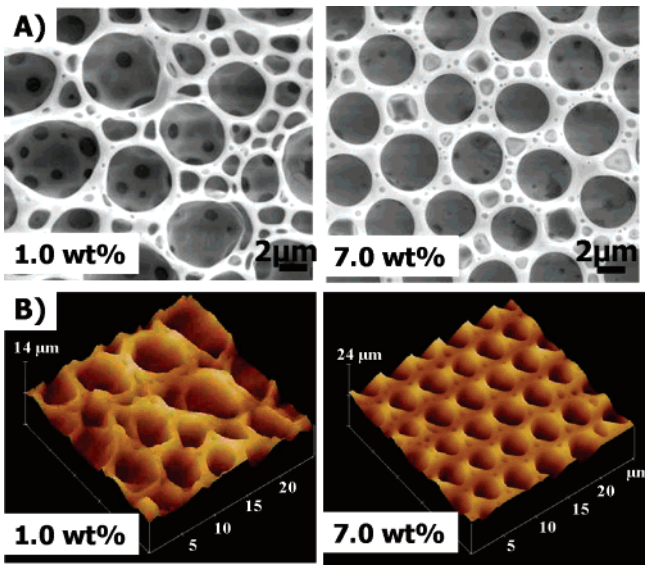

Figure 12. (A) SEM and (B) AFM images of microporous structures developed on the surfaces of a 58 000 g/mol star PDLLA-UM at 76% RH and concentrations of 1.0 and 7.0 wt %.

PDLLA-UM, a four-arm star-shaped PDLLA with methacrylate end groups and an adjacent urethane segment (Scheme 1). The IEM functionalization was performed to obtain star PDLLA-based polymers with photoreactive terminal groups for subsequent cross-linking reactions. Additionally, the urethane moiety was incorporated to provide hydrogen bonding interactions to potentially improve the mechanical properties of the free-standing photo-cross-linked microporous thin films.

FTIR confirmed the successful incorporation of the urethane moiety and methacrylate group as shown in Figure 11. Complete disappearance of the OH absorbance and concurrent appearance of the NH stretch were clearly discerned in the PDLLA-UM sample, supporting quantitative functionalization. Furthermore, the PDLLA-UM showed an additional carbonyl absorbance consistent with a urethane carbonyl as well as an alkene C═C stretch at 1640 cm^{-1} absent in the PDLLA. ^{1}H NMR spectroscopy also confirmed quantitative functionalization as reported in our earlier literature.[40]

Microporous-structured films were developed on the photo-functional PDLLA-UM at concentrations ranging from 1.0 to 7.0 wt % and 76% RH. 4.0 wt % photoinitiator, DMPA, was added to each of the solutions prior to fabrication of the microporous structures. The structured film morphology improved greatly as the concentration was increased from 1.0 to 7.0 wt % (Figure 12), and pore dimensions decreased linearly with

(50) Stenzel, M. H. *Aust. J. Chem.* **2002**, *55*, 239−243.
(51) Xu, Y.; Zhu, B.; Xu, Y. *Polymer* **2005**, *46*, 713−717.
(52) Stenzel, M. H.; Davis, T. P.; Fane, A. G. *J. Mater. Chem.* **2003**, *19*, 2090−2097.
(53) Lin, C.; Tung, P.; Chang, F. *Polymer* **2005**, *46*, 9304−9313.

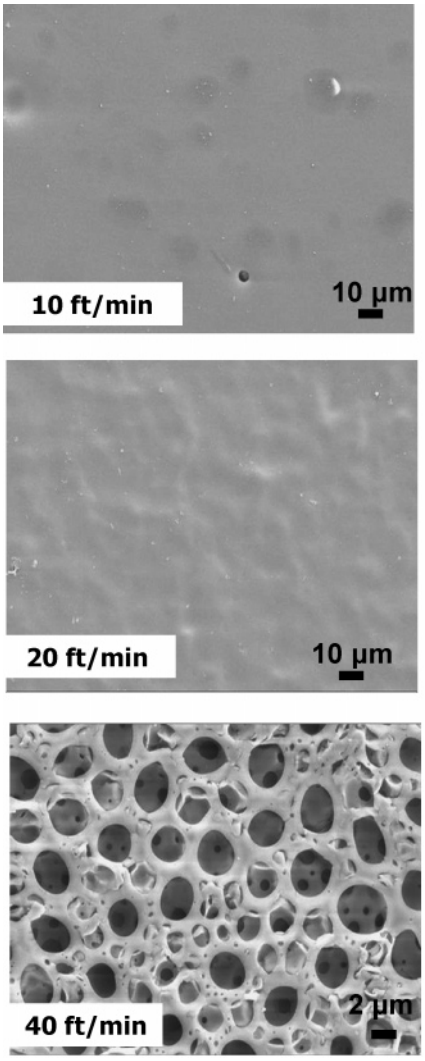

Figure 13. SEM images of star PDLLA-UM microporous-structured film (58 000 g/mol, 7.0 wt %) when photo-cross-linked at belt speeds of 10, 20, and 40 ft/min.

increasing polymer solution concentration in agreement with the trends observed earlier with the nonfunctionalized PDLLA microporous thin films. The presence of smaller pores between the micron-sized pores was observed for the PDLLA-UM films. It is also noted the PDLLA-UM structured films were less ordered than the nonfunctionalized PDLLA structured films at the same concentration. This suggested that modification of the star PDLLA to introduce both methacrylate and urethane units affected the pattern.

To develop cross-linked microporous-structured thin films, the star PDLLA-UM samples were passed through an 1800 W Fusion UV system at a wavelength of 360 nm, the absorption of the photoinitator DMPA. The 7.0 wt % 58 000 g/mol PDLLA-UM polymer was utilized in the cross-linking experiments, as this polymer solution gave the best highly ordered microporous-structured thin films at this particular concentration and molar mass. Several samples were prepared at this concentration and molar mass and cross-linked using the Fusion UV system. The belt speeds were varied at 10, 20, and 40 ft/min to optimize the photo-cross-linking conditions. The temperature of the film surface was measured using a Raytek portable infrared thermometer as 30 °C, with the slight increase in temperature relative to ambient conditions attributed to infrared heating during photo-cross-linking as well as heat release associated with the conversion of π-bonds in the methacrylic groups. Porous structures were not preserved when the films were photo-cross-linked at 10 and 20 ft/min (Figure 13). Hence, the long exposure of the structured polymer film to the UV light at 10 and 20 ft/min allowed the film to soften and collapse onto itself, thereby destroying the ordered structures. However, at 40 ft/min, the pores were preserved due to the short UV exposure time. The glass transition temperatures of the star PDLLA-UM polymers prior to cross-linking were approximately 47 °C; however, after cross-linking, the glass transition temperatures only increased slightly to 55 °C, as measured by differential scanning calorimetry.

The PDLLA-UM films photo-cross-linked at 40 ft/min were extracted in chloroform for 2 h to assess the degree of photo-cross-linking. The photo-cross-linked films were insoluble in chloroform, and the structures were retained. Free-standing microporous-structured PDLLA-UM thin films with gel contents ranging from 99 to 100% were obtained upon drying for 24 h at ambient temperature. It is also presumed, on the basis of our earlier literature that urethane hydrogen bonding will contribute to more durable films. The mechanical properties of the free-standing photo-cross-linked structured films is currently under investigation in our laboratories.

Conclusions

Highly ordered honeycomb porous structures or breath figures were successfully fabricated on well-defined four arm star-shaped PDLLA surfaces. The average pore dimensions decreased with increasing PDLLA solution concentration while an increase in the pore dimensions was observed as the PDLLA molar mass was increased. Additionally, a linear relationship was observed between relative humidity and average pore dimensions. Microporous-structured thin films were also prepared on a star IEM-functionalized PDLLA (PDLLA-UM) with photoreactive pendant groups. Subsequent photo-cross-linking rendered the PDLLA-UM structured films insoluble in chloroform. These permanent PDLLA-based textured films could find potential applications in biomedical sensors and as scaffolds for tissue engineering.

Acknowledgment. This material is based upon work supported by the U.S. Army Research Laboratory and the U.S. Army Research Office under contract/grant number DAAD19-02-1-0275 Macromolecular Architecture for Performance Multidisciplinary University Research Initiative (MAP MURI).

LA0603020

NO. OF
COPIES ORGANIZATION

1 (PDF ONLY) DEFENSE TECHNICAL INFORMATION CTR
DTIC OCA
8725 JOHN J KINGMAN RD
STE 0944
FORT BELVOIR VA 22060-6218

1 US ARMY RSRCH DEV & ENGRG CMD
SYSTEMS OF SYSTEMS INTEGRATION
AMSRD SS T
6000 6TH ST STE 100
FORT BELVOIR VA 22060-5608

1 DIRECTOR
US ARMY RESEARCH LAB
IMNE ALC IMS
2800 POWDER MILL RD
ADELPHI MD 20783-1197

3 DIRECTOR
US ARMY RESEARCH LAB
AMSRD ARL CI OK TL
2800 POWDER MILL RD
ADELPHI MD 20783-1197

ABERDEEN PROVING GROUND

1 DIR USARL
AMSRD ARL CI OK TP (BLDG 4600)